

# Effects of Tower Grounding System Models on Insulation Coordination of Overhead Transmission Lines

A. P. Sakis Meliopoulos  
School of Electrical and Computer Engineering  
Georgia Institute of Technology  
Atlanta, GA 30332-0250

William Adams and  
Robert Casey  
Georgia Power Company  
P. O. Box 4545  
Atlanta, GA 30302

**Abstract:** The lightning performance of overhead transmission lines is measured with the probability of backflashover. This probability is affected by: (a) tower type, (b) grounding arrangement, (c) soil resistivity, and (d) lightning activity and lightning parameters of the area. This paper presents an integrated model of transmission towers, tower grounding and overhead line conductors. The model is utilized in a Monte Carlo simulation for the purpose of predicting the lightning performance of a transmission line. The paper presents the models and the simulation method. Typical results for typical transmission towers and grounding arrangements are provided. The model reveals that the grounding arrangement as well as the surge impedance of the transmission tower are important parameters affecting line performance.

## 1. Introduction

In most locations around the globe, the performance of medium voltage overhead transmission lines is primarily determined by lightning. When lightning terminates on the shield wire of a line, an overvoltage develops across the phase insulators which may lead to a flashover. This mechanism is well understood. Consider Figure 1 for example. The indicated lightning will initiate nine surges, two on the shield wire, six on the phase wires, and one on the downlead conductor, leading to the tower ground. The last surge, reaches the tower ground where it is reflected. If the tower ground surge impedance is low, the reflected surge will be of opposite polarity and when it reaches the top of the tower will mitigate the overvoltage resulting from the lightning current. The voltage of the phase conductors with respect to the tower determine whether a flashover will occur. This voltage depends on the surge characteristics of the tower ground, the surge impedances of the shield wire, tower and phase conductors and the lightning magnitude and rise time. While proper models for overhead circuits and tower have been developed, models for grounding systems lack the necessary attention despite their importance. This paper presents a proper ground model for lightning performance analysis of overhead lines. The grounding model is based on segmenting the ground conductors into segments of typically two to three feet long. Subsequently, the step response of the conductively transferred voltages as well as the step response of the inductively produced voltages are computed by solution of Maxwell's equations. The step responses are used in a time domain simulation of the entire system comprising the tower, its ground and the overhead conductors. A Monte carlo simulation is utilized for generating the distribution of lightning overvoltages

along the line insulator strings. The method can be used to provide the relative merits of various transmission towers and grounding configurations. The paper presents the models and the analysis procedure. It also provides representative results.

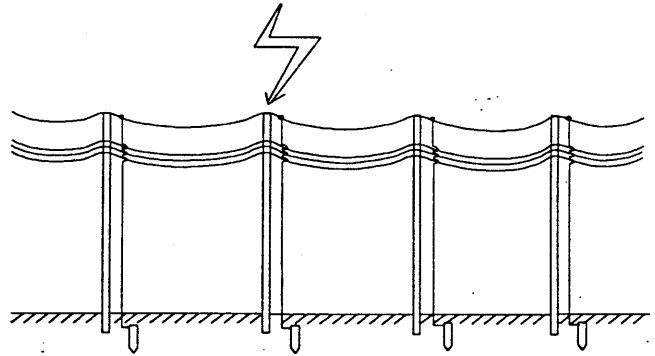


Figure 1. Transmission Line with Tower Grounding

## 2. Model Description

The system under consideration is shown in Figure 1. It is an overhead transmission line suspended on towers. Each tower has a grounding system which may consist of ground rods, counterpoises, etc. The overhead circuit is modeled with standard techniques introduced many years ago. [5], [6]. A frequency dependent model with line asymmetry is used [8]. The grounding system has a rather complex behavior under transient conditions. The grounding model is described in this section in more detail.

Consider a system of buried conductor illustrated in Figure 2. The system is partitioned into  $N$  small segments. Consider two such segments  $k$  and  $j$ . Assume a unit step current is flowing in segment  $j$ . The flow of this current induces voltage on every segment of the grounding system. If the conductor segment  $j$  belongs to an earth electrode, electric current can also flow from the surface of the segment into earth. The flow of this current transfers voltage (by conduction) to every segment of the grounding system. Figure 3a illustrates a typical waveform of the average induced voltage on conductor segment  $k$  due to a unit step electric current through conductor segment  $j$ . Similarly, Figure 3b illustrates a typical waveform of the average transferred voltage to a conductor segment due to a unit step electric current flowing from the surface of the conductor segment  $j$  into earth. The step responses of Figure 3 have been

named Voltage Distribution Functions (VDFs) because they provide the average voltage of a given conductor segment due to a specific unit step current source. The exact form of the VDFs depends on soil resistivity and permittivity, conductor segment dimensions, orientation, etc. They are computed by direct solution of Maxwell's equations in the semi-infinite conducting medium of the earth. The computational procedure is described in Appendix A.

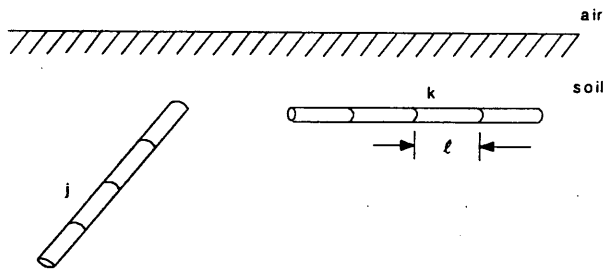


Figure 2. Segmentation of Ground Electrodes

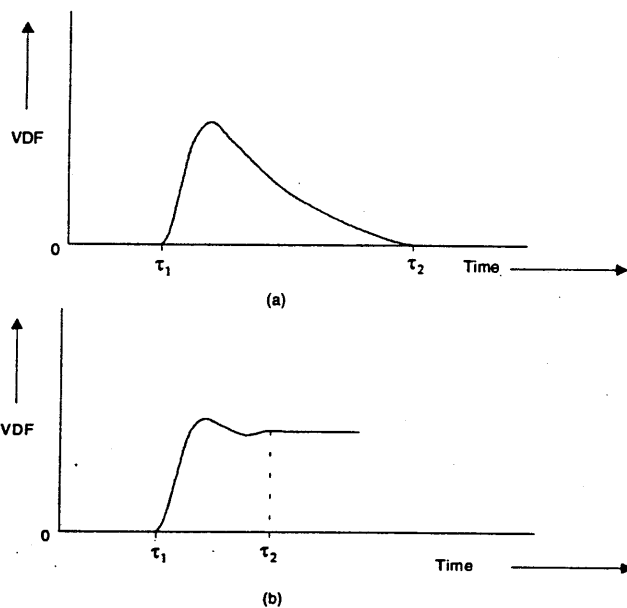


Figure 3. Typical Voltage Distribution Functions Between Two Conductor Segments

- (a) No conductive path between conductor segments
- (b) Existence of a conductive path between conductor segments (i.e. soil)

Note that the general form of the VDFs exhibits a time delay  $\tau_1$ , and a settling time  $\tau_2 - \tau_1$ . The constant value, to which the VDF settles, is zero if there is no conducting medium between the two conductor elements, and nonzero if there is conducting medium (soil) between the two conductor segments.

Once the VDFs have been computed for any pair of conductor segments, then system theory procedures are used for the

analysis of voltages and currents in a grounding system due to an arbitrary excitation. For example, the average voltage on segment  $k$  is obtained by superposition of the contributions from the currents of all segments:

$$e'_{kj}(t) = \sum_{j=1}^N i_{js}(t) * \frac{d}{dt} \text{VDF}(k, j, t), \quad k = 1, 2, \dots, N \quad (1)$$

where

- \* represents the convolution integral
- $e'_{kj}(t)$  is the average voltage of the element  $k$  as a function of time induced by the earth current  $i_{js}(t)$  emanating from the surface of the element  $j$ .
- $\text{VDF}(k, j, t)$  is the VDF between segment  $k$  and  $j$  at time  $t$ .

For numerical computations, Equation (1) is discretized using an integration time step  $h$  and the trapezoidal integration rule. The final equation is in terms of  $e'_{kj}(t)$ ,  $i_{ks}(t)$ , and electric currents at times prior to time  $t$ , i.e.,  $t-h$ ,  $t-2h$ , etc. In other words, the only quantities appearing in time  $t$  are  $e'_{kj}(t)$  and  $i_{ks}(t)$ . Solution of the equation for the electric current  $i_{ks}(t)$  yields:

$$i_{ks}(t) = g_k e'_{kj}(t) + I'_k(t-h, t-2h, \dots) \quad (2)$$

where

- $g_k$  is a constant resulting from the voltage distribution function at time  $t = 0$ ,  $\text{VDF}(k, k, 0)$ ,
- $I'_k(t-h, t-2h, \dots)$  is a quantity depending on the voltage distribution functions  $\text{VDF}(k, m, t)$  and past history current  $i_{ms}(t-h)$ ,  $i_{ms}(t-2h)$ , etc., where  $m = 1, 2, \dots, N$ .

The above described model considers the effects of electromagnetic wave propagation through the soil. In addition, electromagnetic waves propagate through the ground conductors themselves. In order to account for this effect, each conductor segment is modeled as a transmission line with certain parameters. Specifically, consider a ground conductor segment. For symmetry, this conductor segment is partitioned into two transmission lines as it is illustrated in Figure 4 together with the model of equation (2). Note that equation (2) has been given a simple interpretation as a resistive equivalent circuit illustrated with the conductance  $g_{\text{earth}}$  and the current source  $I'_k$ . The two transmission lines LL-ISEG and ISEG-LS are modeled as frequency dependent line models, similar to the model described in reference [4]. The analysis is computationally intensive. However, for short lengths of conductor half segments, as is the case here, a simplified and efficient computational procedure has been devised based on a combination of Snelson transformation and recursive convolutions. The results of this procedure are given next. The derivation of the equivalent circuit of Figure 5 is described next.

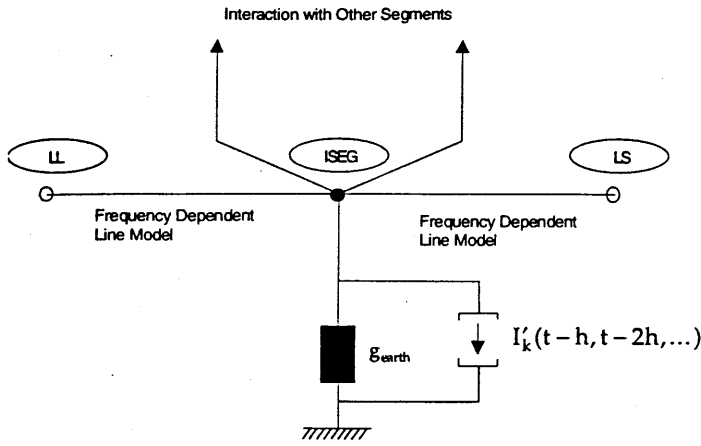


Figure 4. Conductor Segment Model

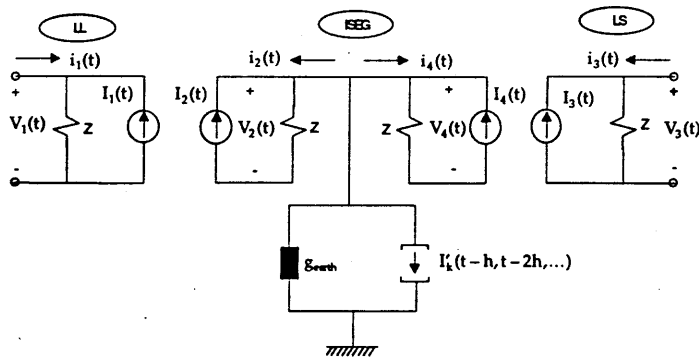


Figure 5. Equivalent Circuit of the Conductor Segment Model

First, the Snelson transformation is applied to the terminal voltages and currents:

$$f_1(t) = v_1(t) + Z i_1(t) \quad (3)$$

$$f_2(t) = v_2(t) + Z i_2(t) \quad (4)$$

where  $Z$  is an arbitrarily selected resistance. It is expedient to select  $Z$  as the limit of the characteristic impedance as frequency goes to infinity. The currents  $i_1(t)$ ,  $i_2(t)$  are the terminal currents flowing into the transmission line at the two ends. The voltages  $v_1(t)$ ,  $v_2(t)$ , are the voltages at the two ends of the transmission line with respect to ground. Next the frequency dependent model of a transmission line is recalled [5]:

$$i_1(t) = Yv_1(t) + I_1(t) \quad (5)$$

$$i_2(t) = Yv_2(t) + I_2(t) \quad (6)$$

where

$$I_1(t) = -Y \int_0^t \alpha_2(\tau) f_1(t-\tau) d\tau - Y \int_0^t \alpha_1(\tau) f_2(t-\tau) d\tau \quad (7)$$

$$I_2(t) = -Y \int_0^t \alpha_1(\tau) f_1(t-\tau) d\tau - Y \int_0^t \alpha_2(\tau) f_2(t-\tau) d\tau \quad (8)$$

$\alpha_1(t)$  and  $\alpha_2(t)$  are the inverse Laplace transformation of  $A_1(s)$  and  $A_2(s)$ ,

$$A_1(s) = \frac{2Z}{D(s)}$$

$$A_2(s) = \frac{(-Z^2 Y_0 + Z_0) \sinh(st_0)}{D(s)} \quad (9)$$

$$D(s) = 2Z \cosh(st_0) + (Z^2 Y_0 + Z_0) \sinh(st_0)$$

The functions  $\alpha_1(t)$  and  $\alpha_2(t)$  in equations (7) and (8) are the weighting functions introduced by Meyer and Dommel [5].

At time  $t$  the quantities  $I_1(t)$  and  $I_2(t)$  are known since they depend on voltages and currents at time  $\tau < t$ . Thus they must be considered constants. Then, equations (5) and (6) represent the equivalent circuit for the ground conductor segment which is illustrated in Figure 5. An efficient computational method for  $I_1(t)$  and  $I_2(t)$  is used based on a recursive evaluation of the convolution integral adopted from Semlyen [9]. Specifically, the current sources  $I_1(t)$  and  $I_2(t)$  are computed with the recursive formula as follows:

$$I(t) = \begin{cases} \delta I(t-h) + \sigma v(t-kh) + \mu v(t-(k+1)h) + \omega v(t-(k+2)h) & \text{if } t > t_0 \\ 0 & \text{if } t \leq t_0 \end{cases} \quad (10)$$

where

$$\delta = e^{-ah}$$

$$\sigma = \frac{b}{a} \left( \frac{1-e^{-ah}}{a^2 h^2} - \frac{3-e^{-ah}}{2ah} + 1 \right)$$

$$\mu = \frac{b}{a} \left( -2 \frac{1-e^{-ah}}{a^2 h^2} + \frac{2}{ah} - e^{-ah} \right)$$

$$\omega = \frac{b}{a} \left( \frac{1-e^{-ah}}{a^2 h^2} - \frac{1+e^{-ah}}{2ah} \right)$$

$$k = \frac{t_0}{h}, \quad h \text{ is the simulation time step.}$$

Above  $I(t)$  can be either  $I_1(t)$ , or  $I_2(t)$ .

The above model is combined with the models of all the other segments of the system under consideration. The end result is an equivalent circuit representation of the combined earth/earth embedded conductor segments that constitute the grounding system. This circuit is excited with an injected electric current at a specified node. Analysis of the equivalent circuit provides the voltage at any node of the circuit. For this purpose, the well known nodal analysis is applied iteratively to provide the transient voltage at any node of the grounding system at time points which are multiples of a selected time step.

In summary, the described model of a grounding system is based on a time domain simulation of the earth embedded conductors. The result is the transient voltage at any point along the ground conductors for any given excitation of the system.

### 3. Monte Carlo Simulation

The overall model of the overhead circuit and grounding system is used in a Monte Carlo simulation to determine the probability

distribution function of the overvoltage. The overall procedure is illustrated in Figure 6. Note that for a specific design, lightning parameters as well as soil resistivity is allowed to vary in accordance to known distribution functions. For each sample, the effects analysis determines the possibility of flashover by comparing the actual stress to the withstand curve of the insulators. A sample of an effects analysis is illustrated in Figure 7. The figure shows the transient voltage across the insulator of phase A superimposed on the time-volt withstand curve of the tower insulation. The indicated waveforms will be interpreted as leading to a flashover. The overall results are reported in two forms: (a) as maximum overvoltage vs probability, and (b) as number of expected flashovers per 100 miles per year versus the tower ground resistance.

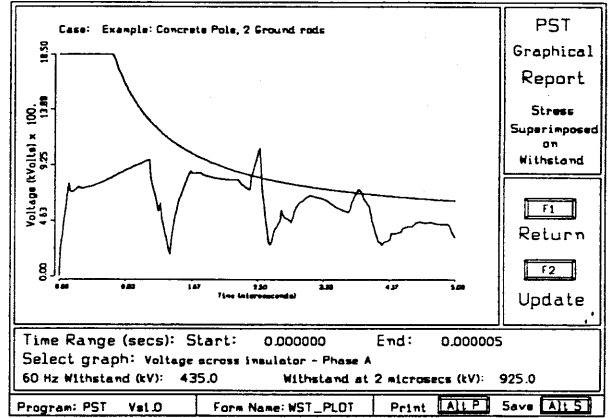


Figure 7. A Sample of Transient Voltage Across the Insulation of Phase A and the Withstand Capability of the Insulator

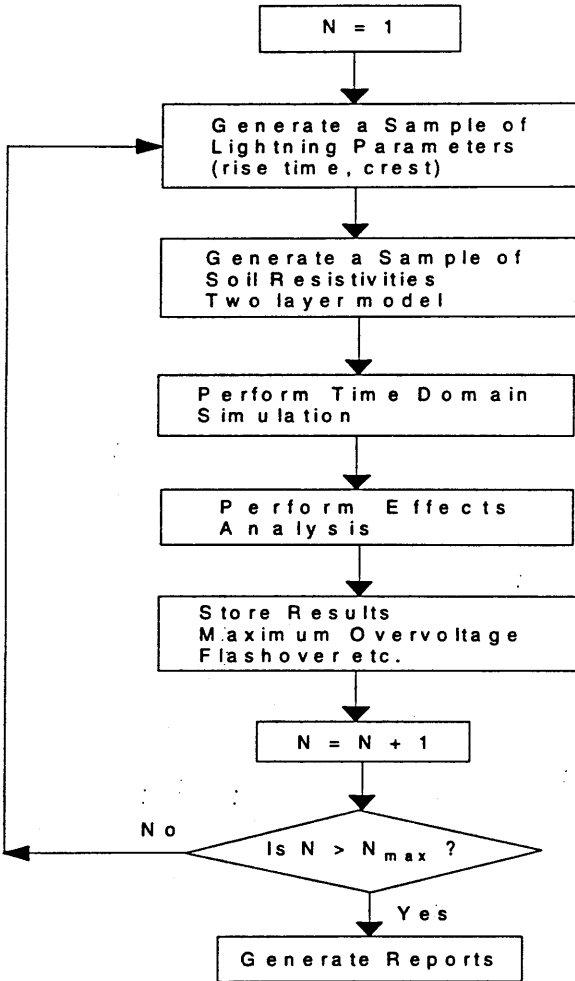


Figure 6. Flow Chart of Monte Carlo Simulation

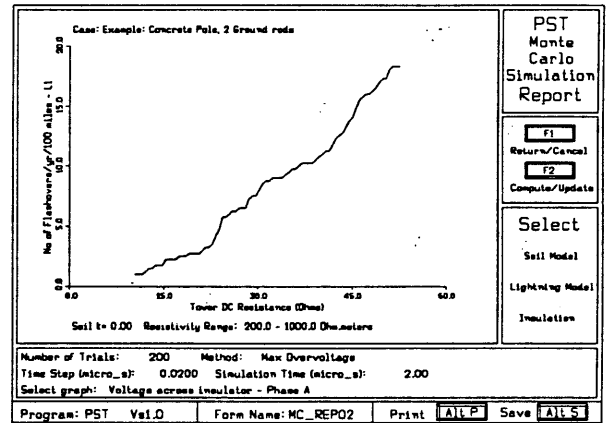


Figure 8. Typical Results of Line Performance Evaluation

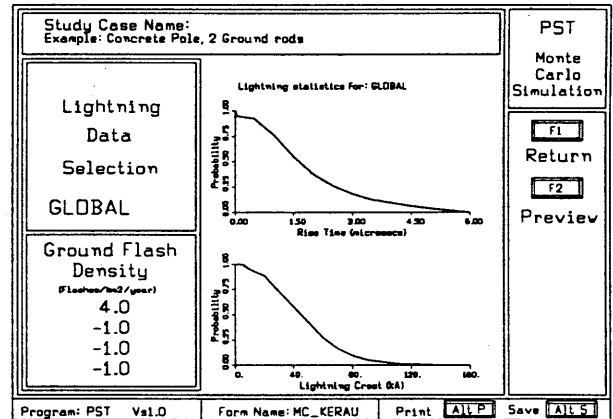


Figure 9. Probability Distribution of Lightning Parameters

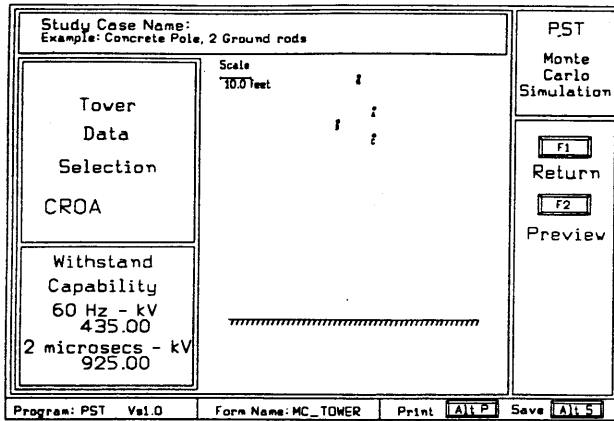


Figure 10. Tower Configuration and Withstand Capability

#### 4. Typical Results

A typical result is illustrated in Figure 8. The figure illustrates the expected number of flashovers per 100 miles of line versus the DC ground resistance of the tower. The results of Figure 8 has been obtained assuming (a) the probability distribution functions (inverted) of lightning rise time and crest value illustrated in Figure 9 and a ground flash density of 4 flashes per km<sup>2</sup> per year, and (b) the tower configuration of Figure 10 with time-volt withstand capability equal to

$$V_w(t) = \begin{cases} 435 + \frac{925-435}{t(\mu s)} 2(\mu s) \text{ (kV)} & t > 0.7 \mu s \\ 1835 \text{ (kV)} & t < 0.7 \mu s \end{cases}$$

The tower grounding arrangement consists of two forty feet long ground rods spaced 20 feet.

It should be apparent that such results can be generated for a variety of tower designs and grounding arrangements - A comparative evaluation of these results leads to selection of optimal designs, improved performance and substantial savings.

#### 5. Conclusions

An integral model of overhead transmission lines, towers and tower grounds has been presented. The model is used in a Monte Carlo Simulation algorithm for the purpose of evaluating the expected lightning performance of specific transmission line design. The model has been utilized in optimizing the tower ground designs of the Georgia Power Company.

#### Reference

1. A. P. Meliopoulos, G. J. Cokkinides, and J. Dunlap, 'Analysis DC Grounding Systems', *IEEE Transients on Power Delivery*, vol. PWRD-3, no. 4, pp. 1595-1604, October 1988.

2. A. P. Meliopoulos and M. G. Moharam, 'Analysis of Grounding Systems', *IEEE Transaction on Power Apparatus and Systems*, vol. PAS-102, no. 2, pp. 389-397, February 1983.
3. A. D. Papalexopoulos and A. P. Meliopoulos, 'Frequency Dependent Characteristics of Grounding Systems', *IEEE Transactions on Power Delivery*, vol. PWRD-2, no. 4, pp. 1073-1082, October 1987.
4. A. P. Meliopoulos, *Power System Grounding and Transients*, Marcel Dekker Inc., New York, 1988.
5. W. S. Meyer and H. W. Dommel, "Numerical Modeling of Frequency-Dependent Transmission-Line Parameters in an Electromagnetic Transients Program," *IEEE Transactions on Power Apparatus and Systems*, vol. PAS93, no. 5, pp.1401-1409.
6. J. K. Snelson, "Propagation of Traveling Waves on Transmission Line - Frequency Dependent Parameters," *IEEE Transactions on Power Apparatus and Systems*, vol. PAS91, no. 1, pp. 85-91, Jan-Feb 1972.
7. P. Anderson, *Analysis of Faulted Power Systems*, Iowa State University Press, Ames, Iowa, 1973.
8. G. J. Cokkinides and A. P. Meliopoulos, "Transmission Line Modeling with Explicit Grounding Representations", *Electric Power Systems Research*, vol 14, no. 2, pp 109-119, April 1988.
9. A. Semlysen and A. Dabuleany, "Fast and Accurate Switching Transient Calculations on Transmission Lines with Ground Return Using Recursive Convolutions", *IEEE Transactions on Power Apparatus and Systems*, vol PAS-94, no. 2, pp 561-571, March/April 75.

#### Appendix A

**Computation of the VDFs:** This appendix presents the computational procedure for the Voltage Distribution Functions (VDFs). The approach is based on solution of Maxwell equations in the frequency domain and subsequent transformation into the time domain. The earth soil is assumed to be a simple conductive medium with conductivity  $\sigma$ , permeability  $\mu$ , and permittivity  $\epsilon$ . It is also assumed that there are charge sources  $\rho_s$  and electric current sources  $\vec{J}_s$ . First, the field quantities (electric field intensity  $\vec{E}$  and magnetic field intensity  $\vec{H}$ ) are computed in terms of the sources  $\rho_s, \vec{J}_s$ . The electric field intensity  $\vec{E}$  is given by the following equation:

$$\vec{E} = -j\omega\vec{A} - \nabla\phi \quad (A.1)$$

where the scalar potential  $\phi$  and the vector potential  $\bar{A}$  are the solution to the following nonhomogeneous Helmholtz equations:

$$\nabla^2 \phi + \gamma^2 \phi = -\frac{1}{\epsilon} \rho_s \quad (\text{A.2})$$

$$\nabla^2 \bar{A} - \gamma^2 \bar{A} = -\mu_0 \bar{J}_s \quad (\text{A.3})$$

assuming the Lorentz condition:

$$\nabla \cdot \bar{A} = -\mu(\sigma + j\omega\epsilon)\phi \quad (\text{A.4})$$

where

$$\gamma^2 = -\omega^2 \mu \epsilon + j\omega \mu \sigma = (\alpha + j\beta)^2$$

$\omega$  : angular frequency (rad/sec)

$\alpha$  : attenuation constant ( $\text{m}^{-1}$ )

$\beta$  : phase constant (rad/m)

Equation (A.1) states that an electric field intensity can arise both from accumulations of charge, through the  $-\nabla\phi$  term, or from time changing magnetic fields, through the  $j\omega\bar{A}$  term.

Once  $\bar{A}$  is known, then the field quantities ( $\bar{E}$ ,  $\bar{H}$ ) are obtained by:

$$\bar{E} = -j\omega\bar{A} + \frac{1}{\mu_0(\sigma + j\omega\epsilon)} \nabla(\nabla \cdot \bar{A}) \quad (\text{A.5})$$

$$\bar{H} = \frac{1}{\mu} \nabla \times \bar{A} \quad (\text{A.6})$$

Assuming that a fixed reference point R is known (typically taken to be much further than the area of interest, i.e., remote earth), the electric potential at a point r in the earth is  $\phi(r)$  computed from:

$$\phi(r) = -\int_R^r \bar{E} \cdot d\bar{l} \quad (\text{A.7})$$

The value of the integral (A.7) is decomposed into two components  $\phi_s(r)$  and  $\phi_a(r)$  with the aid of Eq. (A.5)

$$\phi(r) = \phi_s(r) + \phi_a(r)$$

where

$$\phi_s(r) = -\int_R^r (-j\omega\bar{A}) \cdot d\bar{l} \quad (\text{A.8})$$

$$\phi_a(r) = -\int_R^r \frac{1}{\mu(\sigma + j\omega\epsilon)} \nabla(\nabla \cdot \bar{A}) \cdot d\bar{l} \quad (\text{A.9})$$

The value of the integral (A.9) depends only on the points R and r, i.e., it is independent of the path of integration. Since the integral involves a complex number, the quantity  $\phi_a(r)$  comprises a resistive and a reactive component. The value of the integral of Eq. (A.8) is dependent on the path of integration. This term can drastically increase the complexity of the model. Fortunately, however, the value of  $\phi_s(r)$  becomes substantial only at very high frequencies, To simplify the model, the term

$\phi_s(r)$  is neglected. This simplification is known as the quasi-static approximation. It introduces an error in the computation of the potential which is a function of the frequency and the size of the grounding system. In other words, the quasi-static approximation limits the validity of the developed models in a certain frequency range. Theoretical as well as experimental investigations have demonstrated that the error is only a few percentage points in a very wide range of frequencies for typical grounding systems.

The function  $\phi_s(r)$  computed for an assumed step function  $\bar{J}_s$  (see Eq. (A.3)) is the VDF.